Theoret. Appl. Mech., Vol.35, No.1-3, pp. 191–214, Belgrade 2008

A plastic collapse method for evaluating rotation capacity of full-restrained steel moment connections

Kyungkoo Lee, * **Bozidar Stojadinovic** †

Abstract

An analytical method to model failure of steel beam plastic hinges due to local buckling and low-cycle fatigue is proposed herein. This method is based on the plastic collapse mechanism approach and a yield-line plastic hinge (YLPH) model whose geometry is based on buckled shapes of beam plastic hinges observed in experiments. Two limit states, strength degradation failure induced by local buckling and low-cycle fatigue fracture, are considered. The proposed YLPH model was developed for FEMA-350 WUF-W, RBS and Free Flange connections and validated in comparisons to experimental data. This model can be used to estimate the seismic rotation capacity of fully restrained beam-column connections in special steel moment-resisting frames under both monotonic and cyclic loading conditions.

Keywords: Steel structures; moment connections; rotation capacity; low-cycle fatigue; plastic collapse mechanism; seismic design

1 Introduction

Fully-restrained connections between beams and columns in steel moment-resisting frame structures built in the US were closely scrutinized after the 1994 Northridge earthquake because of their unexpectedly poor performance

*Department of Architectural Engineering, Seoul National University, Seoul, 151-742, Korea, e-mail: kklee21@snu.ac.kr

†Department of Civil and Environmental Engineering, University of California at Berkeley, Berkeley, CA 94720, USA, e-mail:boza@ce.berkeley.edu

during that earthquake. These investigations are summarized in the FEMA-350 report [1]. Furthermore, this report presents new design recommendations for fully-restrained connections in steel moment-resisting frame structures. At the core of these design recommendations is requirement that connections in Special Steel Moment Resisting Frames (SMRF) have a total rotation capacity exceeding 4% radian while maintaining strength above the nominal plastic capacity of the beam or loosing no more than 20% of the maximum connection resistance. To demonstrate this, a pre-qualification test requirement was imposed in the design codes. Thus, each new connection type is required to pass a pre-qualification test conducted using a prescribed procedure. Such pre-qualification test approach was adopted and codified in FEMA-350 [1] and AISC [2] documents because rotation capacity of steel moment connections could not be reliably predicted using conventional analytical models, such as finite element or fracture mechanics models. Even though this approach is safe, it is expensive and it hampers development of new connection designs.

During a severe earthquake only few cycles of large deformation may be sufficient to cause failure of steel structural components sensitive to low-cycle fatigue. Failure of pre-qualified steel moment connections after only a few cycles of high-amplitude deformation was observed in pre-qualification tests as ductile tearing of the metal in the creases of the beam buckled shape in the plastic hinge region. While low-cycle fatigue resistance is not an explicit requirement of the connection pre-qualification test procedure, resistance to this failure mode is important for seismic structural design because steel structures may have to endure a number of significant earthquakes, each having a few cycles of large deformation demand that may pose a cumulative connection fracture risk.

In this paper we propose, develop and validate an analytical method to predict failure of connections due to buckling and low-cycle fatigue and estimate their seismic rotation capacity in special steel moment resisting frames under both monotonic and cyclic loading conditions. The proposed method uses a plastic collapse approach and a yield-line model of a beam plastic hinge. A yield-line plastic hinge (YLPH) model was originally developed by Gioncu and Petcu [5,6] to model local buckling of a beam in a moment connection under monotonic loading. This method, based on interpretation of experimental evidence on the shape of the buckled plastic hinge region, is extended to random cyclic loading appropriate for seismic analysis. Both strength degradation failure induced by local buckling of beams and low-cycle fatigue failure caused by plastic strain accumulation at critical points in the plastic hinge region are considered. YLPH models for common US post-Northridge connections, such as the WUF-W, the RBS and the Free Flange connection, are constructed and applied to compute the seismic rotation capacity of these connections. Thus, the YLPH is validated by comparison to experimental data.

2 Background

Well-designed US post-Northridge connections that satisfy pre-qualification test criteria are likely to undergo local buckling before they exhaust their available rotation capacity. Rotation capacity of a beam-column connection has been defined as the rotation when the strength of the connection is either below the nominal plastic strength of the beam section or bellow 20% of the maximum resistance of the connection. Kemp [3] introduced a relation between rotation capacity and parameters of beam section, such as flange slenderness, web slenderness and lateral-torsional slenderness. Stojadinovic et al.[4] also investigated comprehensively a local and lateral-torsional buckling of wide-flange beams in unreinforced steel moment connections. The effects of beam flange and web slenderness, lateral supports, and axial deformation restraint on the plastic rotation capacity of the connection were described there.

It has been observed that plastic behavior of steel under cyclic loading is nonlinear and depends on the load history. Furthermore, the stress-strain response of steel changes significantly with cyclic straining into the plastic range. Thus, fatigue life in the plastic range may be more accurately described as a function of the cyclic strain amplitude than the cyclic stress amplitude. Low-cycle fatigue test data for a family of different constant strain amplitude tests are usually displayed using a logarithmic plot of strain amplitude versus the number of cycles to failure at that amplitude (Manson-Coffin's rule). These plots will typically show an approximately linear relation between the number of cycles to failure and strain amplitude in the log-log space.

Gioncu and Petcu [5], Anastasiadis et al. [6], and M?ller et al. [7] introduced the yield-line concept to model the buckled shapes of typical I-shape steel beam sections observed in experiments. They also used a plastic work approach to define a collapse mechanism and thereby determine the rotation capacity of European H-section beams under monotonic loading. Finally, they showed that the yield-line model produced post-peak strength degradation rates and rotation capacities in good agreement with monotonic-loading test results. The YLPH model we present herein extends their method to various connection types and provides a systematic approach to model the post-buckling behavior of steel moment connections under both cyclic and monotonic loading.

3 Yield-Line Plastic Hinge Model

Inelastic local buckling of the flange and/or the web of compact steel W-shape cross-sections typical for US construction develops after substantial yielding and strain hardening. In steel moment frames, such yielding is assumed to occur only in the plastic hinge region of the beams. The principal assumption

of this study is that such local buckling is confined to the beam, and that the column or the panel zone of the connection does not buckle locally. This assumption is supported by observations made in numerous connection subassembly tests conducted after the 1994 Northridge earthquake. A substantial majority of these tests have shown that local flange buckling was followed by local web buckling: this assumption is maintained throughout this study. Elastic local buckling is not considered in this study as it is assumed that customary cross-section slenderness criteria are adhered to. Deformation capacity of the beam plastic hinge will, therefore, depend on the rotation enabled by the local buckling mechanism of the beam section in the plastic hinge region that takes shape after local buckling occurs.

The yield-line mechanism is developed following the guidelines proposed by Gioncu and Petcu [5]. Lateral-torsional buckling is not considered: only in-plane local buckling of the cross-section elements is assumed to occur. It is conservatively assumed that local flange buckling and local web buckling occur at the same time and interact with each other. Individual occurrence of one of these two local buckling events would require more work by external forces and would, thus, result in an un-conservative estimate of plastic hinge resistance.

The topology of the yield lines and plates is defined by the locally buckling-deformed shape of a beam plastic hinge observed during tests. The beam cross-section is discretized into uni-axial fibers whose length is defined by the geometry of the yield-line model. The buckled shape is treated as an initial imperfection for the fibers in compression and is used to compute their critical stress. Using the buckled shape geometry, the kinematics of the yield-line mechanism is derived to relate a beam plastic hinge rotation increment to an increment of yield-line rotation and flange and web axial shortening in the entire cross section of the plastic hinge. A relation between external and internal forces acting on the yield-line plastic hinge fibers is derived using the principle of virtual work. The principle of virtual work (a weak form of equilibrium of the yield-line moments and axial forces in the plastic hinge) is formulated to compute the effective stress distributions in the buckled region. The complete stress distribution is integrated across the entire cross-section area. The cross-section model is iterated on the buckled flange displacement until equilibrium between internal and external forces is achieved. Finally, the available rotation capacity is computed using force or deformation limit state criteria. The force limit state defines critical strength degradation, either below the nominal plastic strength or below 80% of the maximum beam section strength. The deformation limit state defines fracture initiation in the plastic hinge when ultimate tensile strain is attained at a critical point of a critical yield-line in the buckled region.

3.1 Prerequisites of the Model

In order to relate beam plastic hinge rotation capacity to low-cycle fatigue fracture at the creases of the YLPH model, total beam plastic hinge rotation is assumed to comprise two components, as shown in Figure 1: 1) rotation before local buckling θ^{FCS}, which will be determined by axial fiber cross section model using classical bending theory; and 2) rotation after local buckling θ^{YLPH}, which will be modeled using a yield-line plastic mechanism.

Two additional assumptions are made. First, initiation of local buckling corresponds to maximum bending resistance of the plastic hinge M_{pr}. This assumption implies all other sources of capacity loss, such as lateral-torsional buckling or brittle fracture, are not occurring. Second, the entire post-buckling rotation is modeled by the yield-line plastic mechanism. Thus, the contribution of the classical Bernoulli's bending theory mechanism to total beam rotation is neglected after local buckling starts.

The length of the beam plastic region is set as the length of the flange buckling wave which is computed using Lay's [8] equation. Assuming the flange yields fully (across its entire cross section) before inelastic local buckling starts and considering rotational restraint provided by the web against flange local buckling, Lay computed the wavelength of the flange buckle corresponding to the minimum critical buckling stress. An expression for the probable peak plastic hinge moment resistance at a plastic hinge M_{pr} (FEMA-350 Ch3 equation (3-1) [1]) was used to compute the critical stress to initiate flange local buckling of the flange, consistent with our first assumption. Thus, an elastic-perfectly plastic stress-strain constitutive relation for the fibers in the part of the YLPH model in compression is defined.

3.2 Geometry and Kinematics

The geometry of the yield-line plastic hinge model for a typical W-shape beam section under monotonic benidng is shown in Figure 2. Geometric assumptions and constraints are: 1) flange and web buckling wavelengths, L_f and L_w, remain unchanged during plastic rotation; 2) flange remains perpendicular to the web during plastic hinge rotation; 3) the joint between the flange and the web is fully restrained; and 4) sections on either side of the plastic hinge (defined by the buckling wavelength) remain plane after deformation.

A yield-line mechanism deformation relation was developed as follows [9]:

1. The flange buckling wavelength L_f was computed using Lay's equation and the web buckling wavelength L_w was computed from geometry using similar triangles;

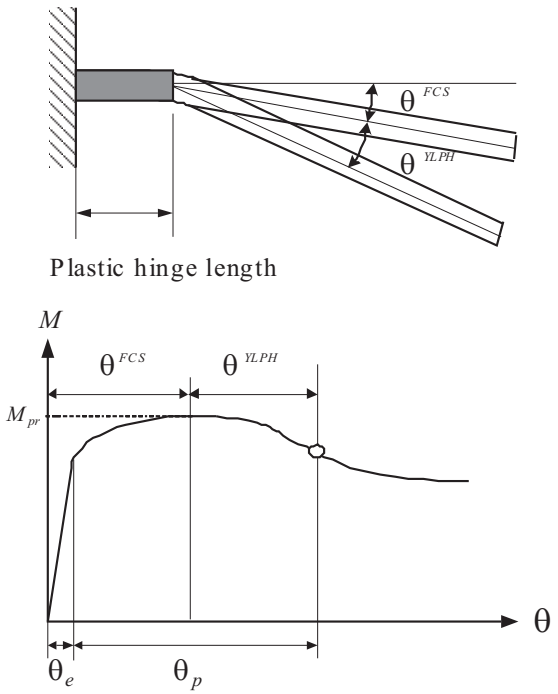

Figure 1: Rotaiton components of a beam plastic hinge

2. Using Pythagoras' Theorem, flange and web buckling amplitude, U_f and U_w were expressed in terms of yield-line mechanism displacement and L_f and L_w;

3. Assuming that the flange and the web twist to keep the flange perpendicular to web, flange buckling amplitude was related to web buckling amplitude; and

4. Location where maximum web buckling amplitude occurs was obtained by geometry regardless of the magnitude of plastic hinge rotation increment.

Flange and web yield-line mechanisms within a plastic hinge include the plastic zone, where axial shortening occurs, and the yield lines, where plastic rotation occurs. Axial deformations of the flange and the web yield-line mechanisms after buckling are shown in Figure 2. Plastic zones are shown in gray, while the thick lines represent the yield lines. Consider an axial deformation of a fiber strip in yield-line mechanisms. Such axial deformation may be decomposed into shortening in the plastic zone and rigid body motion caused by yield-line rotations. From kinematics, the incremental rotations corresponding to the perpendicular and inclined yield lines, $\Delta\theta_1^{YL}$ and $\Delta\theta_2^{YL}$, respectively, can be related to the increment of axial displacement [7]. Consider the fibers of

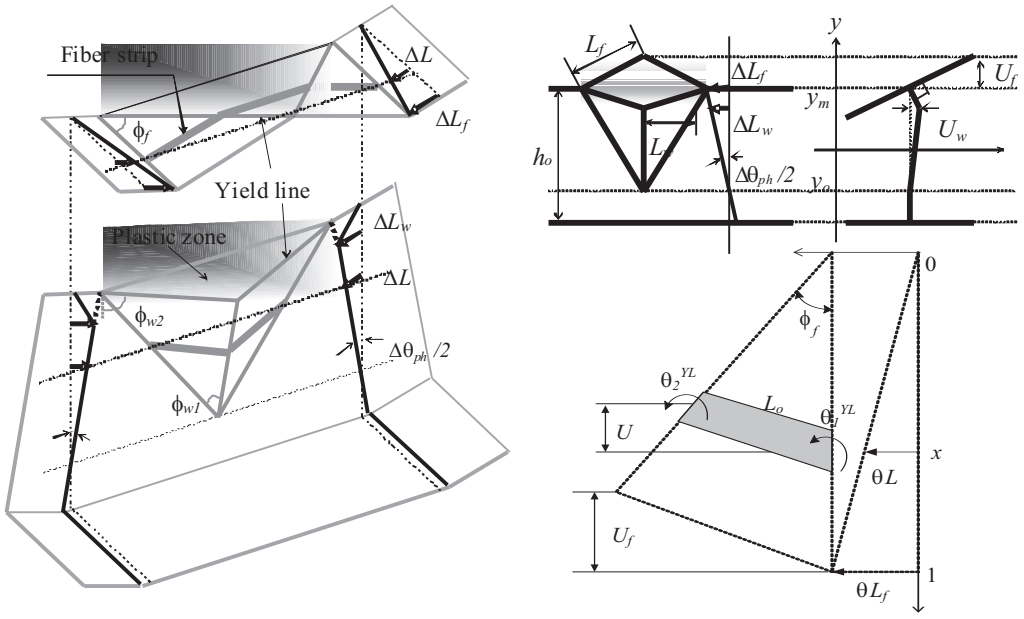

Figure 2: YLPH model geometry and the kinematics of a fiber in the YLPH model under monotonic loading

the buckled web next. The web buckled shape mechanism has two parts. The upper part includes the plastic zone and the yield lines, while the lower one comprises only the yield lines. Rigid body motion of fibers and the corresponding yield-line rotations can be determined following the same procedure [7]. Finally, for both flange and web local buckling, the increments of flange and web buckling amplitudes can be related to the increment of axial displacement ΔL and yield-line rotations $\Delta\theta_i^{YL}$ as follows:

$$\begin{bmatrix} \Delta\theta_1^{YL} \\ \Delta\theta_2^{YL} \end{bmatrix} = \begin{bmatrix} A_1 \\ A_2 \end{bmatrix} \cdot \frac{\Delta L}{U} \tag{1}$$

where the geometric transformation matrix is defined as

$$\begin{bmatrix} A_1 \\ A_2 \end{bmatrix} = \begin{bmatrix} 1 \\ 1/\cos\phi_f \end{bmatrix} \text{ for a flange fiber}$$

$$= \begin{bmatrix} 1/\cos\phi_{w1} \\ 1/\cos\phi_{w2} \end{bmatrix} \text{ for a web fiber that folds in the plastic hinge}$$

$$= \begin{bmatrix} 1/\cos\phi_{w1} \\ 1 \end{bmatrix} \text{ for a lower web fiber that does not fold}$$

and U is the buckling amplitude of a fiber. Angles ϕ_f, ϕ_{w1}, and ϕ_{w2} are the angles of the inclined yield lines to the yield lines at the end of the fibers (perpendicular to beam axis) where axial deformation is being applied, as shown

in Figure 2.

Under cyclic loading, two buckling shapes must be considered. If the flange that buckled in compression straightens completely when it goes into tension, such that there is no residual buckling shape, as shown in Figure 2, a relation between a yield-line mechanism displacement ΔL and rotation under loading and reverse loading can be obtained as if the loading was monotonic. If, on the other hand, the flange that buckled does not straighten completely when in tension, a residual buckled shape, shown in Figure 3, must be considered. In this case, the relation between ΔL and $\Delta\theta_{ph}$ can be obtained by a superposition of two mirror-image monotonic buckling shapes, one for each side of the beam, as:

$$\begin{aligned} \Delta L &= \Delta L^T + \Delta L^B \\ \Delta\theta_{ph} &= \Delta\theta_{ph}^T + \Delta\theta_{ph}^B \end{aligned} \tag{2}$$

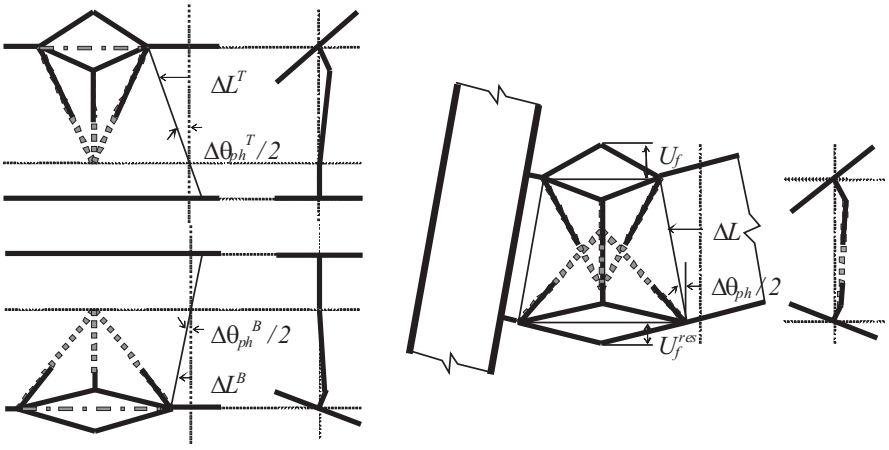

Figure 3: Cyclic YLPH model with a residual buckling shape under reversed cyclic loading

3.3 Principle of Virtual Work

Consider a fiber strip of unit width and thickness t, and a yield-line mechanism shown in Figure 4. Assuming an elastic-perfectly plastic moment-curvature relation for a yield line cross-section, the plastic bending moment per unit length of the yield line is $m_p = F_y^* t^2/4$. This plastic moment is assumed to act along the entire length of all yield lines in this yield-line mechanism. The work of the axial force on the axial deformation of the fiber strip is external.

Internal work is assumed to be done by the bending moments working on yield-line rotations and by the axial force working on axial shortening of the plastic zones between the yield lines. Since axial deformation is composed of shortening and rigid body rotation, the principle of virtual work can be expressed as:

$$N \cdot \Delta L = \sum_{i=1}^{2} m_p \cdot \Delta\theta_i^{YL} \tag{3}$$

where N is an externally applied axial force over a unit width of the fiber strip. Then, the axial force is obtained by inserting Equation (1) into Equation (3) as follows:

$$N = \frac{m_p}{U} \cdot (A_1 + A_2) \leqslant F_y^* t \tag{4}$$

where A_1 and A_2 are components of the geometric transformation matrix in Equation (1) and t is the plate thickness in which a fiber strip is formed. Note that A_1 and A_2 and m_p are constants. Because $1/U$ is a non-linear function of ΔL (with ΔL to the power of -0.5) increasing ΔL results in a decreasing N. Thus, internal work due to rotations at yield lines is not increasing as fast as external work by N.

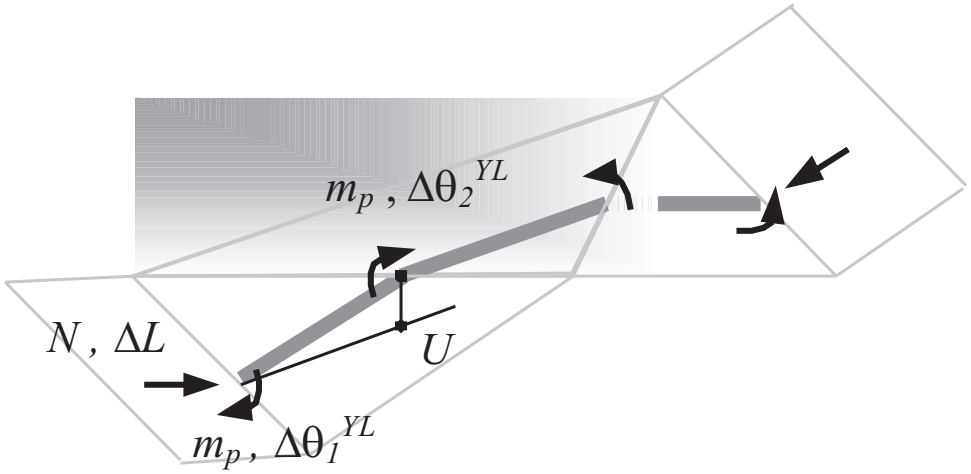

Figure 4: Principle of virtual work on a fiber strip

Before local buckling occurs (i.e. when the axial force N is less than that critical for buckling) virtual work equation can be used, but the rotation-related component of internal virtual work must be discarded. Buckling of a fiber strip occurs when the external axial force reaches a critical value. After local buckling occurs, additional internal virtual work is done along the yield lines

due to large axial and out-of-plane deformation of the fiber strip corresponding to the buckling amplitude. Therefore, the magnitude of the externally applied axial force N on a fiber strip must decrease after buckling (after it reaches the critical buckling value) in order to maintain virtual work equilibrium.

Principle of virtual work applies to both initial loading and subsequent re-loading of the flange in compression, before and after buckling. In-plane deformation before local buckling is elastic. After yielding, external axial force N may be assumed to remain on a "yield plateau" considering that the axial strains are such that strain hardening does not occur. However, after local buckling occurs, the magnitude of the axial force decreases as the magnitude of axial deformation increases. Shortening corresponding to increase of axial deformation may be assumed to be only due to geometric effect. Under cyclic loading, external axial force N under such cyclic deformation is assumed to follow an elastic unloading and reloading path away and toward a yield surface, respectively.

3.4 Cross-Section Forces and Stress Distribution

Aggregated fiber axial forces in a plastic hinge cross section must be in equilibrium with externally applied moment and axial force on the plastic hinge. Fiber axial forces, which can be easily converted to effective axial stresses, are computed using either the fiber strip model described above in the buckled region of the cross section, or the elastic-plastic stress-strain relation for the stable (un-buckled) portion of the cross section. A possible fiber effective stress distribution in a plastic hinge section after buckling is shown in Figure 5. In the buckled portion of the section (labeled Yield-Line in Figure 5), a weak form of equilibrium for the yield-line fiber strips was formulated above to compute the effective fiber stress distribution. Assuming that plane sections remain plane at the boundaries of the yield line plastic hinge mechanism (Bernoulli's assumption), a simple constitutive relation for elastic-perfectly-plastic material was applied to compute the stress distribution in the stable portion of the section (labeled Bernoulli in Figure 5). A candidate stress distribution can be integrated to compute cross-section moment and axial force. These values depend on the location of the center of rotation of the plastic hinge mechanism, defined by a distance y_0 measured from the undeformed section centroid, as shown in Figure 2. Iteration on $y_0$must be conducted to enforce equilibrium between internal fiber forces and external moment and axial force at the YLPH boundary cross section.

Note that as the rotation of the plastic hinge grows, buckling amplitudes in the flange and the web grow according to the YLPH model kinematics to satisfy geometric compatibility internal work on the yield lines increases, resulting in

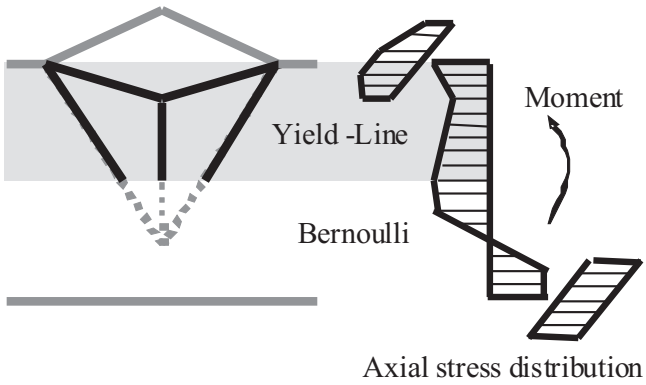

Figure 5: Effective axial stress distribution in a plastic hinge cross section

a reduction of the average compression force in the compressed part of the cross section. This, in turn, causes a reduction in the tensile force, a shift of the neutral axis, a reduction in the moment arm, and a drop in plastic hinge moment resistance. Such behavior is observed in tests.

4 Validation

Validation of the YLPH model is conducted by comparing the data collected during tests of exterior (beam on one side of the column only) fully-restrained moment connection to analytical models of these connections. The tests used to validate the YLPH model are listed in Table 1: all tests were conducted using a pre-qualification test cyclic incrementally increasing drift-based specimen deformation history.

An analytical model of an exterior connection specimen comprised of a rotational spring, a yield-line plastic hinge, and a fiber cross section cantilever beam. The rotational spring represents the elastic behavior of the column and the connection panel zone. A YLPH model determines the moment and rotation of the buckled portion of the beam. Deformation of the stable (not buckled) portion of the beam is calculated using a curvature distribution corresponding to a linear moment distribution over the cantilever span. The curvature of the cantilever sections is computed using a fiber cross-section model in FEDEAS [10]. This was done because some of the cantilever sections may be partially yielded, but not buckled. This fiber cross-section model was analyzed using the force formulation. Newton's method is used for non-linear analysis of the specimen analytical model. The bisection iteration method was used to iterate the YLPH model to converge the post-buckling response. Note that inelastic

panel zone deformation was not considered.

A bilinear material model with strain hardening was used to model the stress-strain relation for the column and the sections in the stable part of the beam. For YLPH model section, an elastic perfectly plastic material model was used with a modified yield stress F_y^* corresponding to the probable peak plastic hinge moment resistance at a plastic hinge M_{pr} computed according to FEMA-350 guidelines.

Table 1: Exterior beam-column connection specimens used to validate the YLPH model

Specimens	Connection Type	Beam Section	Column Section
RC01 [11]	Cover Plate	W30x99 (US)	W14x176 (US)
T5 [12]	WUF-W	W36x150 (US)	W14x311 (US)
SP9.2 [13]	Free Flange	W30x99 (US)	W14x176 (US)
DB600-SW [14]	RBS	H600x200x11x17mm	H588x300x12x20mm
DB700-SW [14]	RBS	H700x300x13x24mm	H428x407x20x35mm

4.1 Comparison of Flange Local Buckling Amplitudes

A specimen RC01 tested by Kim et al. [11] developed a typical local buckle in the beam plastic hinge region. Flange local buckling amplitudes recorded during the first and the second loading cycle at the same speicimen drift level, normalized with respect to the beam flange width, are plotted in Figure 6. Evidently, buckling amplitudes computed using the YLPH model compare well to those measured during the test. The rate of increase of the flange buckling amplitude up to 0.03 radian connection drift angle is in particularly good agreement with the test results. The 0.03 radian drift angle corresponds to the beam nominal plastic strength or strength degradation limit states.

Several important characteristics of local buckling behavior may be related to the buckling amplitudes. First, many connection tests show that strength resistance starts to drop at the connection drift angle greater than approximately 0.02 radians, when local flange buckling and/or local web buckling starts. The amplitudes in Figure 6 start to increase very rapidly at the drift angle of 0.02 radians when flange local buckling occurs and strength degradation starts. Second, after the first cycle at the 0.03 radian drift angle, flange buckling amplitude increase becomes less rapid. This corresponds to the start of connection strength degradation. However, after the second cycle at 0.03 radian drift angle buckling amplitude increases rapidly again. The reason for such behavior may be the residual deformation in the buckled region present

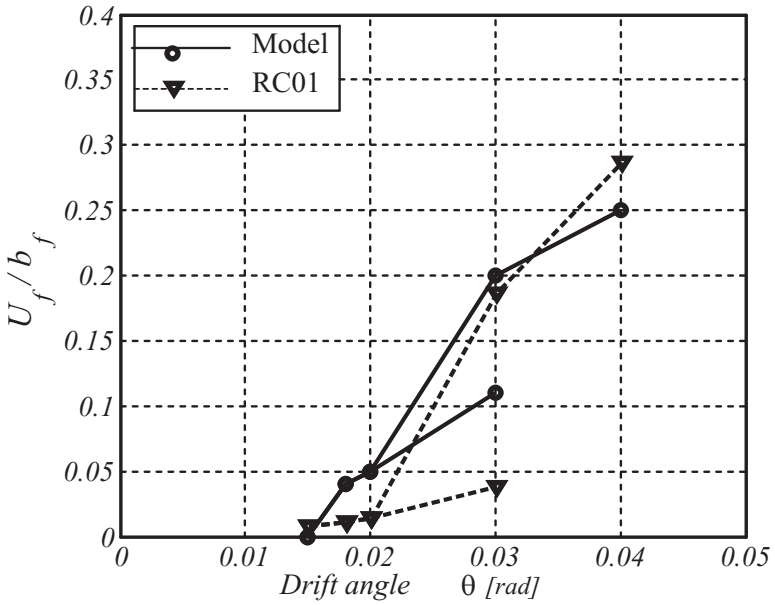

Figure 6: Comparison of first and second cycle flange local buckling amplitudes

before the second loading cycle to the same drift level. Third, the rate of increase of buckling amplitude at the drift angle of 0.04 radians becomes smaller. It was observed that the strength of the connection degraded rapidly at first and then slowed as local buckling progressed. The rate of strength degradation seems to be proportional to that of flange and/or web local buckling amplitude growth rate.

4.2 Comparison of Available Rotation Capacity under Monotonic Loading

Kemp [3] proposed that beam rotation capacity is related to the slenderness ratio for each of the three buckling modes: flange local buckling, web local buckling and lateral-torsional bucking. He suggested an effective slenderness ratio λ_e^{Kemp} to relate available rotation capacity and normalized slenderness ratios based on beam tests under monotonic pure flexure conducted by Kemp [3], Kuhlmann [15], and Lukey and Adams [16]. The effective slenderness ratio and available rotation capacity are related as:

$$\lambda_e^{Kemp} = \left[\frac{h_o}{t_w} \cdot \frac{\gamma_w}{70}\right] \left[\frac{b_f}{2t_f} \cdot \frac{\gamma_f}{9}\right] \left[\frac{L_i}{r_{yc}} \cdot \gamma_f\right]; \quad R_a = \frac{\theta_p}{\theta_e} \tag{5}$$

where normalized yield strength coefficients $\gamma_w = (F_{yw}/36)^{1/2}$ and $\gamma_f = (F_{yf}/36)^{1/2}$ (nominal yield strength of the tested beams was 36ksi (248MPa)). Available

rotation capacity R_a is defined by normalizing plastic rotation capacity θ_p by the elastic rotation corresponding to the plastic strength θ_e (Figure 1). Note that Kemp used the plastic rotation limit beyond which the strength degrades below the plastic strength of the section.

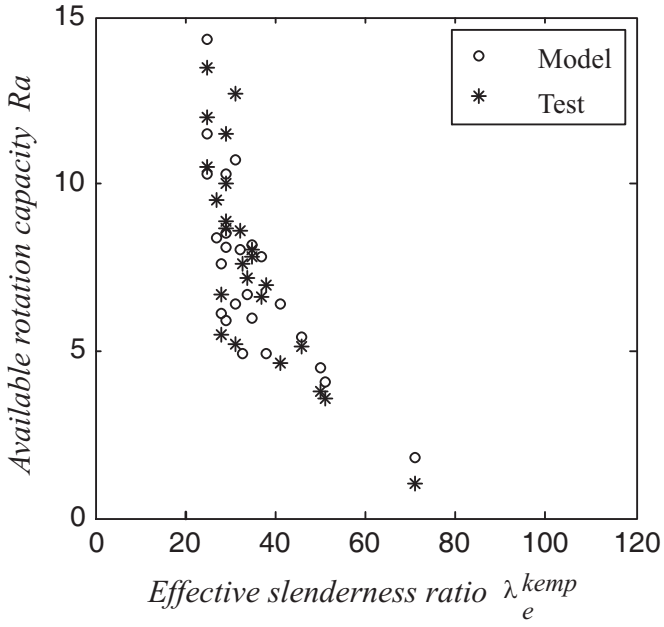

Figure 7: Available rotation capacity of beams under monotonic loading

European shapes used in 24 beam tests conducted by Kuhlmann [15] are used in Figure 7 to validate the YLPH model. Available rotation capacities obtained from the tests and from the YLPH model are plotted: the agreement is reasonable. Note that the relation between the available rotation capacity under monotonic loading and the effective slenderness ratio suggested by Kemp is evident.

4.3 Comparison of Three Connection Types under Cyclic Loading

First, an improved welded unreinforced flange-welded web (WUF-W) connection was modeled to represent specimen T5 tested by Ricles et al. [12]. Figure 8 shows the moment vs. plastic rotation response of this WUF-W connection under cyclic loading. Beam moment at the column face M_f was normalized by the beam nominal plastic strength M_p. Panel zone deformation measured during test was subtracted from the total connection rotation to compare test data with rotation obtained using the YLPH model. It is observed that the

YLPH model produces very rapid strength degradation in the second cycle at the drift level when local buckling initiates. This is mainly because material strain-hardening in the buckled plastic hinge region was not considered in the YLPH model. The proposed model produces a more conservative beam plastic rotation capacity than the test specimen.

Second, a Free Flange connection was modeled to represent specimen 9.2 tested by Choi et al. [13]. Figure 8 shows the response of this connection under cyclic loading. Results of the YLPH model compare well to the test results. The panel zone deformation measured during test was small enough to be neglected. Note that the strength drops predicted by the YLPH model match very well with those from the test for the 0.03 radian drift angle cycles. At the drift angle of 0.04 radians, test strength drops more than model strength because lateral-torsional buckling of the beam occurred. The proposed model gives a conservative rotation capacity according to the strength degradation limit state which is expected to be reached before lateral-torsional buckling occurs in adequately braced beams.

Third, two reduced beam section (RBS) connections were modeled to represent specimens DB600-SW and DB700-SW tested by Lee et al. [14]. Figure 8 shows the moment-rotation response of these connections. Results of the YLPH model compare very well to these test results. Note that the panel zone deformation measured during the test was subtracted from total connection drift angle to compare test data to rotations obtained using the YLPH model. Results of the YLPH model are, again, conservative in terms of drift angle or rotation.

5 Low Cycle Fatigue

The validated YLPH model is now used to relate the FEMA-350 Collapse Prevention limit state to initiation of flange fracture using a low-cycle fatigue limit state. The low-cycle fatigue limit state was formulated at the level of the yield line by monitoring the accumulated strain due to cyclic loading of the model. The tensile strain capacity at the critical yield line of the buckled flange in the YLPH model was conservatively assumed to be 0.2, which corresponds to the ultimate steel strain achieved in monotonic axial tension tests of steel coupons. This strain limit was used in the YLPH model to determine the corresponding number of cycles to failure of the connection under a constant-amplitude drift angle loading history. Note that the YLPH model shows that a constant-amplitude drift angle loading history on a connection sub-assembly results in a cumulatively increasing buckling deformation because of the inability of the buckled flange to straighten leading to an incrementally increasing yield-line

strain amplitude sequence (Figure 9).

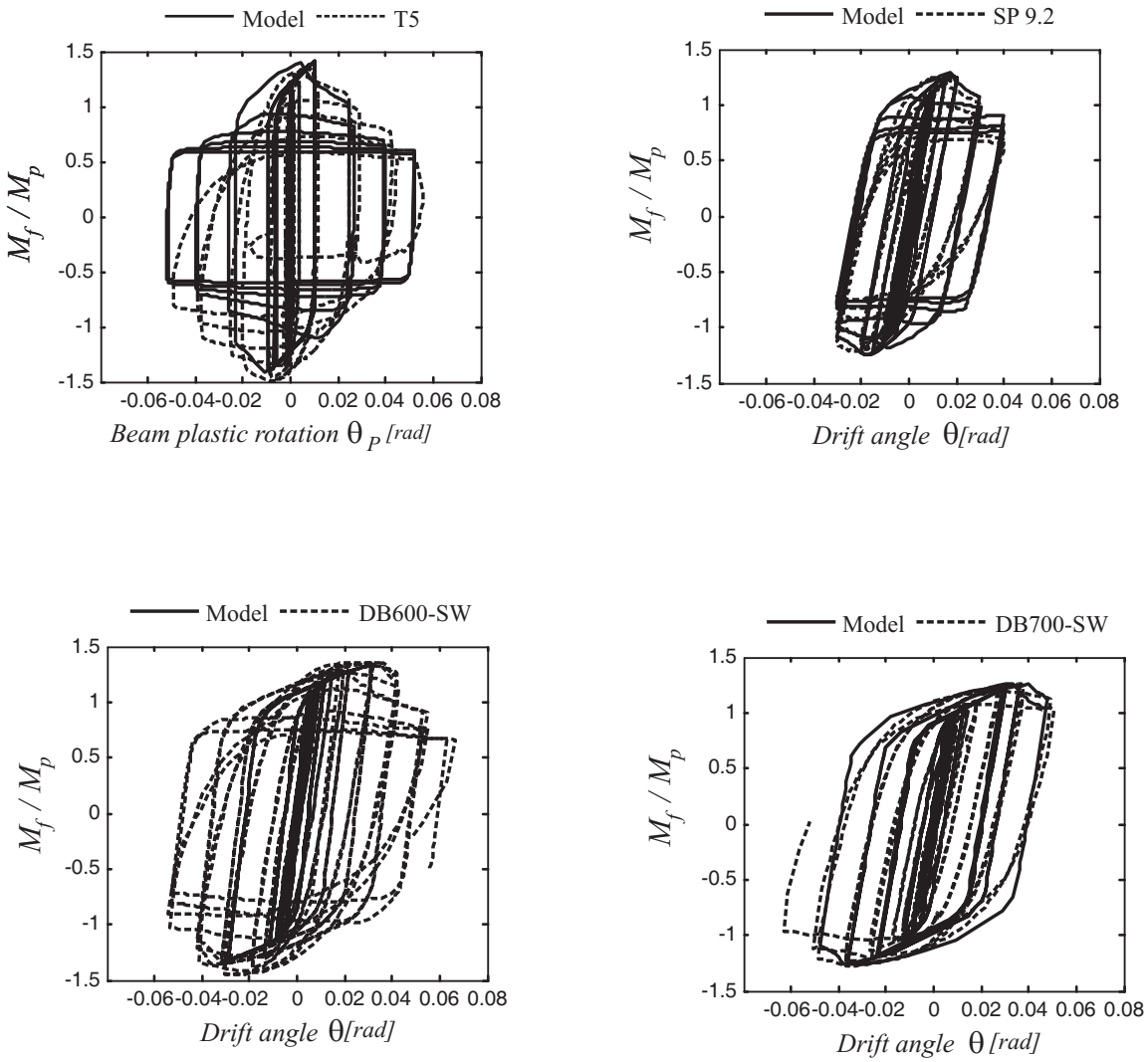

Figure 8: Comparison of YLPH models and connection test data

Using a log-log linear approximation, expected fatigue life may be computed from an $S - N$ curve as suggested by Manson and Coffin as follows:

$$N_f S^m = C \tag{6}$$

where N_f is the number of cycles to failure, S is constant (total or plastic) deformation amplitude, and C and m are material property constants obtained from tests. Experiments show that m has values of approximately 2 for plastic strain amplitudes and approximately 3 for total strain amplitudes [18].

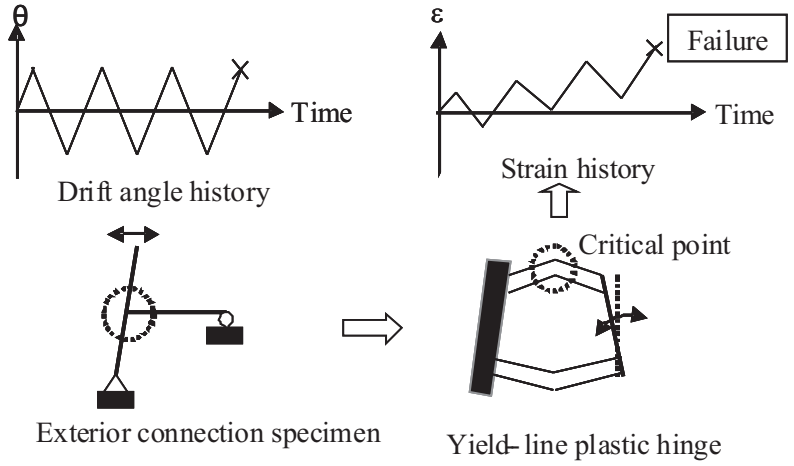

Figure 9: Fatigue strain accumulation and failure of a yield line

5.1 Effects of beam section slenderness

A series of YLPH model analyses of various WUF-W connection specimens listed in Table 2 were conducted at different constant amplitude levels in order to observe how to correlate the number of cycles to failure by ductile tearing at a yield line to connection deformation or rotation amplitude. The YLPH models were subjected to constant-amplitude rotation sequences (at 0.02, 0.025, 0.03, 0.035, and 0.04 radian levels) until failure defined by a low-cycle fatigue material limit state at the critical point on a yield line. Note that the YLPH model can be used to predict low-cycle fatigue failure at a critical yield-line only if the amplitude of cyclic deformation is large enough to initiate local buckling of the beam, i.e., larger than 0.02 radian total rotation. The minimum yield strength value used in these simulations was set to 50ksi (345Mpa) and modulus of elasticity to 29,000ksi (200GPa). The columns in these YLPH models were assumed to be rigid in order to clearly observe the effect of beam section geometry on fatigue life. The effect of varying beam section geometry parameters, such as flange or web slenderness, with respect to the baseline configuration was examined. Slenderness ratios of web and flange for local buckling were normalized using AISC Seismic Provisions for Structural Steel Buildings 2005 Table I-8-1 [17]. When normalized slenderness is larger than one, the cross section element is seismically non-compact. Normalized flange slenderness λ_{fn} and normalized web slenderness λ_{wn} are defined as:

$$\lambda_{fn} = \frac{b_f/2t_f}{0.3\sqrt{E/F_y}} \tag{7}$$

$$\lambda_{wn} = \frac{h/t_w}{2.45\sqrt{E/F_y}} \tag{8}$$

Table 2: WUF-W connection model properties used to investigate their low-cycle fatigue life

Models	D	t_w	b_f	t_f	λ_{fn}	λ_{wn}
W100F100	30in	0.49in	10.5in	0.73in	1.00	1.00
W100F120	30in	0.49in	10.5in	0.61in	1.20	1.00
W100F075	30in	0.49in	10.5in	0.97in	0.75	1.00
W075F100	30in	0.65in	10.5in	0.73in	1.00	0.75
W050F100	30in	0.97in	10.5in	0.73in	1.00	0.50

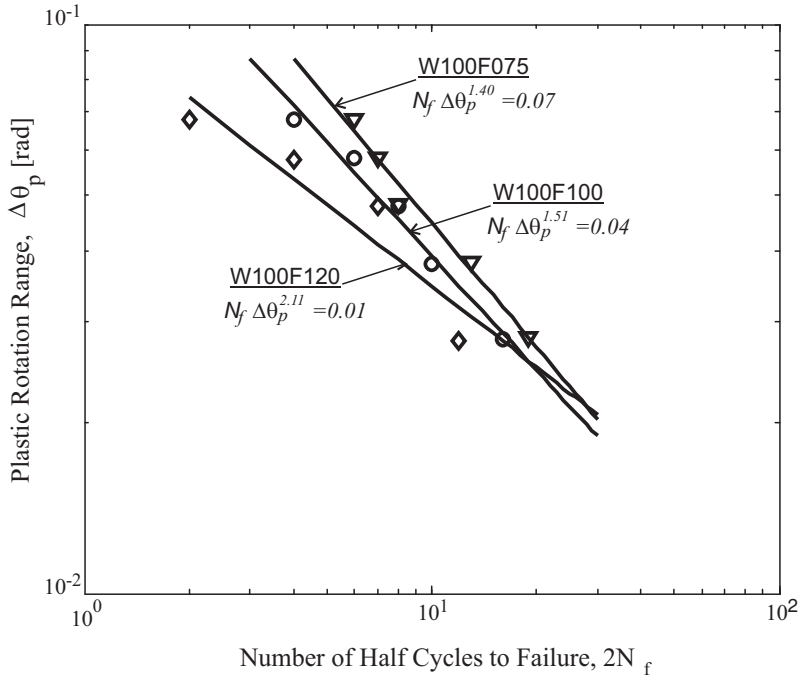

Figure 10: Low cycle fatigue plot for various falnge slenderness values

The low-cycle fatigue behavior of WUF-W connections with different normalized flange slenderness λ_{fn} and web slenderness λ_{wn} ratios is compared in Figures 10 and 11, respectively. Log-log plots of the number of half cycles to failure, $2N_f$, versus the plastic rotation range $\Delta\theta_p$ of a connection sub-assembly are shown. Linear least square fitting of the YLPH model results produced material property value from m = 1.40 to m=2.34 (the slope of the $S-N$ curve) for the plastic rotation range. The data shown in the figures fits the Mason-Coffin equation very well. As expected, sections with less slender (thicker) flanges and

webs have the better fatigue life. Beams with thicker flanges have the better fatigue life under large amplitude plastic rotation demand, shown by the increasing slope of the S-N curves. The beam with very thick web (corresponding to normalized web slenderness of 0.5) showed better fatigue life, but the other two beams with slenderness ratios of 0.75 and 1.0 had almost the same fatigue life, due to the flange governing the fatigue life of these beams.

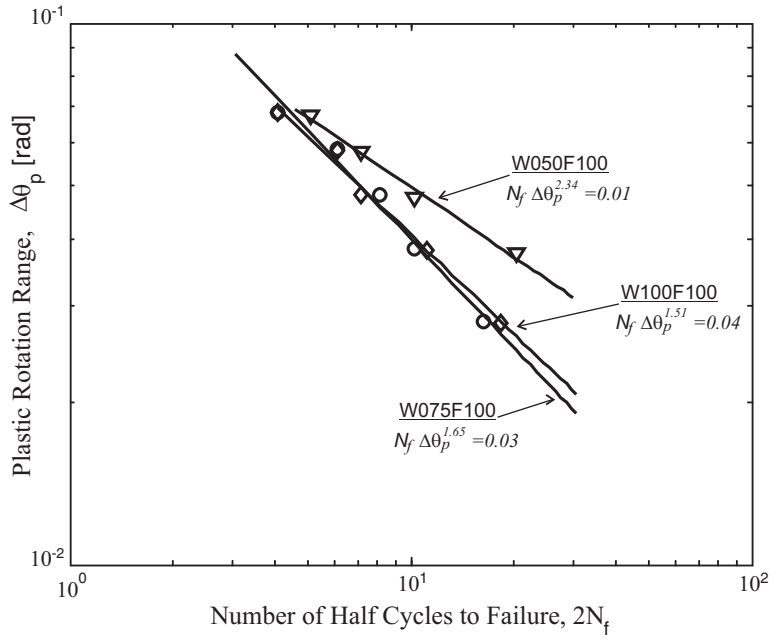

Figure 11: Low cycle fatigue plot for various web slenderness values

5.2 Effects of connection type

The YLPH models for different types of connections were developed and investigated for their low-cycle fatigue life. The FEMA-350 WUF-W, RBS and Free Flange connections were modeled, as shown in Figure 12. Each connection type differs in the location where the plastic hinge forms and in the buckled shape of the plastic hinge. For a WUF-W exterior connection subassembly, a basic YLPH model (W100F100 listed in Table 2) was used. For an RBS connection subassembly, the YLPH model was developed to represent local buckling behavior in the reduced section. Deformation of the portion of the beam between the column and the reduced section was computed using a stable (non-budkling) beam bending behavior model. This deformation cannot be disregarded since it is large after the beam cross section yields. For a Free Flange connection subassembly, a different type of model was developed to rep-

resent its local buckling shape considering the effect of a large shear tab and the free flange length.

Low-cycle fatigue behavior and rotation limit for these connections was investigated using the series of constant-amplitude drift angle sequences, discussed above. The columns were, again, assumed to be rigid. Figure 12 shows a log-log plot of the plastic rotation amplitude versus the number of half cycles to failure for different connections. Again, a Manson-Coffin relation between the plastic rotation amplitude and the number of rotation cycles to failure agrees very well with the computed data. The S-N curves of the three connection types are linear and have slopes of 1.51 for WUF-W, 2.43 for RBS and 2.71 for the Free Flange connection. Thus, different types of connections have a different fatigue life. For example, the Free Flange connections is expected to have the best low-cycle fatigue life of all considered connections, followed by WUF-W and RBS connections under the large amplitude plastic rotation loading.

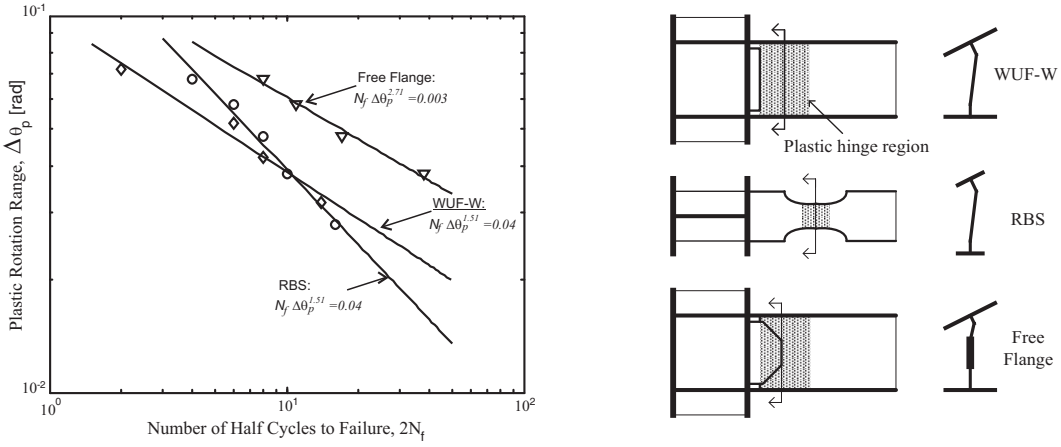

Figure 12: Low cycle fatigue plot for RBS, WUF-W and free flange connections

6 Conclusion

A yield-line plastic hinge (YLPH) model was proposed and developed to investigate the local buckling behavior of beam-column connections under monotonic and cyclic loading. The geometry of the beam plastic hinge after local buckling occurs was modeled using the yield-line approach. A force-displacement relation for the plastic hinge was computed using the principle of virtual work, assuming large deformations at the yield lines. Effective stress distribution in the buckled region was computed using incremental virtual work equilibrium

equation formulated for the assumed yield-line plastic mechanism and iterated to satisfy the force equilibrium of the cross section.

YLPH models for stand-alone cantilever beams and exterior beam-column connection specimens were developed and compared to a number of tests to validate the YLPH modeling approach. The agreements between YLPH model predictions and test data with respect to flange local buckling amplitude under cyclic loading, beam rotation capacity under monotonic loading and moment-rotation response of three FEMA-350 pre-qualified connections are generally very good. The YLPH provided consistently conservative estimates of the available connection rotation capacity.

The yield-line model approach is not commonly used to analyze steel beam-column connections. The finite element method or the fracture mechanics approaches dominated the research practice in the last decade. However, the yield-line plastic hinge model approach has a distinct advantage over other approaches when post-buckling moment-rotation response of a beam-column connection is examined. Even though the yield-line approach does not produce a mechanically completely consistent solution (in the strong equilibrium formulation sense), it offers a sufficiently accurate approximate solution (in the weak equilibrium formulation sense). The YLPH model offers a very good estimate of plastic rotation capacity compared to connection test results. This model effectively captures the onset of local buckling, the buckled shape and the buckling amplitude in typical US moment connections under both cyclic and monotonic loading. The second advantage of the YLPH model approach is that it enables quick and effective conduct of parametric studies across wide ranges of geometry parameters and limit state assumptions to evaluate connection rotation capacity.

One such parametric study was conducted to investigate low-cycle fatigue, an important limit state for seismic structural design of steel fully-restrained beam-column connections because large cumulative local plastic deformation may be induced in them during just a few high-magnitude earthquakes. In this study, a YLPH model, used to compute the strain amplitudes at critical yield line locations, and a low-cycle fatigue failure criterion based on strain accumulation, were coupled to investigate the low-cycle fatigue limit state of beams and connections under cyclic loading. To the best knowledge of the authors, this is the only such model developed to date to investigate low-cycle fatigue of modern US full-restrained moment connections. As expected, longer low-cycle fatigue life is obtained from sections with less slender flanges and webs. More important, a comparison of the FEMA-350 pre-qualified WUF-W, RBS and Free Flange connections indicates that the Free Flange connection may have a longer fatigue life than the other two connection types.

References

[1] FEMA, *Recommended Seismic Design Criteria For New Steel Moment-Frame Buildings*, FEMA Report No. 350, Federal Emergency Management Agency, Washington, D.C., 2000.

[2] AISC, *Manual of Steel Constructions, Load & Resistance Factor Design Specification for Structural Steel Building*, 3rd ed., American Institute of Steel Construction, Inc., Chicago, IL, 2002.

[3] Kemp, A, R, "Inelastic local and lateral buckling in design codes", *Journal of Structural Engineering*, ASCE, Vol. 122, No 4, 1996, pp374-382.

[4] Stojadinovic, B, Goel, S, C, Lee, K, H, Margarian, A, G, and Choi, J-H, "Parametric Tests on Unreinforced Steel Moment Connections", *Journal of Structural Engineering*, ASCE, Vol. 126, No 1, 2000, pp 40-49.

[5] Gioncu, V, and Petcu, D, "Available rotation capacity of wide-flange beam and beam-columns part 1, 2", *Journal of Constructional Steel Research*, Vol 43, No 1-3, 1997, pp 161-244.

[6] Anastasiadis, A, Gioncu, V, and Mazzolani, F, M, "New trends in the evaluation of available ductility of steel members", *Proceedings of Behavior of Steel Structures in Seismic Areas*, 2000, pp 3-26.

[7] Muller, M, Johansson, B, and Collin, P, "A new analysis model of inelastic local flange buckling", *Journal of Constructional Steel Research*, Vol 43, No 1-3, 1997, pp 43-63.

[8] Lay, M, G, "Flange Local Buckling in Wide-Flange Shapes", *Journal of the Structural Division*, ASCE, Vol 91, No 6, 1965, pp 95-115.

[9] Lee, K, and Stojadinovic, B, "Seismic rotation capacity and lateral bracing of US steel moment connections", *Proceedings of Behavior of Steel Structure in Seismic Areas,* 2003; pp 335-342.

[10] Filippou, F, C, *FEDEAS: Finite Element for Design, Evaluation and Analysis of Structure*, Department of Civil and Environmental Engineering, University of California at Berkeley, 2000.

[11] Kim, T, Whittaker, A, S, Gilani, A, S, Bertero, V, V, and Takhirov, S, M, *Cover-Plate and Flange-Plate Reinforced Steel Moment-Resisting Connections*, Pacific Earthquake Engineering Research Center, University of California at Berkeley, Report No. PEER 2000/07, 2000.

[12] Ricles, J, M, Fisher, J, W, Lu, L-W, Kaufmann, E, J, "Development of improved welded moment connections for earthquake-resistant design", *Journal of Constructional Steel Research*, Vol 58, No 5-8, 2002, pp 565-604.

[13] Choi, J, Goel, S, C, and Stojadinovic, B, "Design of Free Flange Moment Connection", *AISC Engineering Journal*, Vol 129, No 1, 2003, pp 25-42.

[14] Lee, C-H, Jeon, S-W, Kim, J-H, and Uang, C, M, "Effects of Panel Zone Strength and Beam Web Connection Method on Seismic Performance of Reduced Beam Section Steel Moment Connections", *Journal of Structural Engineering*, ASCE, Vol 131, No 12, 2005, pp 1854-1865.

[15] Kuhlmann, U, "Definition of flange slenderness limits on the basis of rotation capacity values", *Journal of Constructional Steel Research*, Vol 14, No 1, 1989, pp 21-40.

[16] Lukey, A, F, and Adams, P, R, "Rotation capacity of wide flanged beams under moment gradient", *Journal of Structural Division*, ASCE, Vol 95, No 6, 1969, pp 1173-1188.

[17] AISC, *Seismic Provisions for Structural Steel Buildings*, American Institute of Steel Construction, Inc., Chicago, IL, 2002.

[18] Fisher, J.W, G. L. Kulak and I. F. C. Smith, "A Fatigue Primer for Structural Engineers", National Steel Bridge Alliance, Chicago, IL, May 1998.

Submitted on February 2008.

Odredjivanje rotacionong kapaciteta krutih veza u čelicnim ramovima metodom plastičnog loma

U ovom clanku je predstavljen formalini metod za modeliranje loma plasticnih zglobova formiranih u celicnim gredama zbog lokalnog izvijanja i zamora materiajal. Ovaj metod je zasnovan na teoriji plasticnog loma i na YLPH modelu plasticnog zgloba formiranom od krutih ploca spojenih linijama plasticnog tecenja na osnovu geometrije izivjenih plastiching zglobova testiranih celicnih greda u krutim ramoskim vezama. Lom u predlozenom modelu je moguc po jednom od dva granicna stanja: pad kapaciteta na savijanje zbog lokalnog izvijanja; i lom zbog nisko-ciklicnog zamora materijala. Predstavljen model je razvijen za FEMA-350 WUF-W, RBS i Free Flange krute ramoske veze i potvrdjen uporedjenjem sa eksperimentalnim merenjima. YLPH model moze da se koristi za procenu kapaciteta rotacije krutih ramoskih veza izmedju stubova i greda pod monotonim ili ciklicnim opterecenjem.

doi:10.2298/TAM0802191L Math.Subj.Class.: 74L15, 92C37